



## **Numerical simulation of indoor airflow and particle deposition in the clean room (surgical operation room)**

**Haider M.H. AL-Shami, Ali A. Monem, Emad A. Khazal**

Department of Mechanical Engineering, Engineering College, University of Basra, Basra-Iraq.

Received 25 Dec. 2017; Received in revised form 2 Mar. 2018; Accepted 11 Mar. 2018; Available online 1 May 2018

### **Abstract**

This study presents three-dimensional analysis Lagrangian model (DPM) for particle movement in turbulent indoor airflows inside the clean room (surgical operation room) in al-Najaf hospital in Iraq, to obtain the best appropriate environmental conditions within the room, and to account for the process of particle deposition at solid boundaries. These particles were originated from the supply air. The computations were accomplished with the aid of the computational fluid dynamics (CFD) program, known as ANSYS 15 program using (drift-flux) model. This program was validated against the results of a similar model given by chen. et.al [1], which shows a reasonable matching. The numerical results collected from the surgical operation room were done at different inlet velocities, to state the effect of turbulent inlet airflow velocity on the particles concentration around the room contents (specially the operation table), and to track the paths of these particles.

**Copyright © 2018 International Energy and Environment Foundation - All rights reserved.**

**Keywords:** Clean room (surgical operation room); Indoor air-flow; Particles movement; (deposition); Lagrangian method.

### **1. Introduction**

A cleanroom is defined by ISO14644-1 [2] as “a room in which the concentration of airborne particles is controlled., and which is constructed and used in a manner to minimize the introduction, generation, and retention of particles inside the room, and in which other relevant parameters, e.g. temperature, humidity, and pressure, are controlled as necessary [4].

The objective of clean room technology in various clean room classes in the industrial process, operation room and laboratory rooms are to ensure the control of contaminants in sensitive processes. due to exposure of the product to airborne microbes during processing or if severe sedimentation of airborne microbes can occur on critical process surfaces, clean room technology can be used to solve the problems [5, 6]. In an aseptic clean room, the air flow, properly filtered, is flushed from the top of the chamber to special grids placed at the bottom of the structure. Then, it is recirculate by an air filtering unit; here, part of the air flow is ejected and replaced by external air that will undergo filtration. A main requirement of clean rooms is that they are maintained at a pressure higher than the external one, to prevent pollutants air flow from the environment. Currently accepted standards describing clean rooms are developed by ISO (2006) [2].

Chen, F. et, al. [1] developed a three-dimensional drift-flux model for particle movements in turbulent indoor airflows, and combined it into Eulerian approaches to account for the process of particle deposition

at solid boundaries with three typical ventilation systems and velocity variation as a function of particle size was observed. The movements of submicron particles were like tracer gases while the gravitational settling effect should be taken into account for particles larger than 2.5  $\mu\text{m}$  and it was found the advantageous principle for gaseous pollutants that a relatively less-polluted occupied zone existed in DV(displacement ventilation and UFAD (under-floor air distribution) was also applicable to small particles.

Junjie Liu et, al. [3] used computational fluid dynamics (CFD) simulation method [1]. The investigation was focused mainly on the influence of the medical lamps and the thermal plume with different airflow patterns around the critical zone under the horizontal air supply system. Ultra clean air was supplied from a fan filter unit. The patient and surgeon were assumed to be releasing 200 and 400 particles per minute, respectively. The results showed that when the air supply and return facilities were installed on the same lateral wall to keep a state of horizontal flow ventilation in the OR, medical lamps and the thermal plume had no obvious influence on the horizontal airflow patterns around the critical zone in the (surgical operation room).

The current study predicts the indoor air flow distribution and particle movement inside a surgical operation room in al-Najaf hospital using a computational fluid dynamics (CFD) program known as ANSYS 15 program. The flow is assumed to be unsteady-state turbulent flow, and the particles are originated through the inlet air flow. The Lagrangian model (DPM) is used to state the effect of turbulent inlet air flow velocity on the particles concentration around the room contents (specially the operation table), and to track the paths of these particles.

## 2. Theroy: (Governing equations)

### 2.1 Navier stock equations

The instantaneous equation of mass, momentum, and energy conservation are presented in the following:

#### Conservation of mass:

Rate of increase of mass in fluid element = Net rate of flow of mass into element

Taking  $U$ ,  $V$  and  $W$  to be the velocity components in the  $x$ ,  $y$  and  $z$  directions respectively, ( $\rho$ ) the fluid density and ( $t$ ) the time, then the rate of increase in the density ( $\rho dx dy dz$ ) within the control volume  $dx dy dz$  equals the net rate of influx of mass to the control volume.

$$\frac{\partial u}{\partial x} + \frac{\partial v}{\partial y} + \frac{\partial w}{\partial z} = 0 \quad (1)$$

#### The momentum equations:

Rate of increase of momentum of fluid particle = Sum of forces on fluid particle

X-direction (U momentum):

$$\rho \left( u \frac{\partial u}{\partial x} + v \frac{\partial u}{\partial y} \right) = X - \frac{\partial P}{\partial x} + \mu \left( \frac{\partial^2 u}{\partial x^2} + \frac{\partial^2 u}{\partial y^2} \right) \quad (2)$$

Y-direction (V momentum):

$$\rho \left( u \frac{\partial v}{\partial x} + v \frac{\partial v}{\partial y} \right) = Y - \frac{\partial P}{\partial y} + \mu \left( \frac{\partial^2 v}{\partial x^2} + \frac{\partial^2 v}{\partial y^2} \right) \quad (3)$$

Z-direction (W momentum):

$$\rho \left( u \frac{\partial w}{\partial x} + v \frac{\partial w}{\partial y} \right) = Z - \frac{\partial P}{\partial z} + \mu \left( \frac{\partial^2 w}{\partial x^2} + \frac{\partial^2 w}{\partial y^2} \right) \quad (4)$$

#### The total energy equation:

Rate of increase of energy of fluid particle= Net rate of heat added to fluid particle- Net rate of work done on fluid par

$$\rho C_p \left( u \frac{\partial T}{\partial x} + v \frac{\partial T}{\partial y} \right) = K \left( \frac{\partial^2 T}{\partial x^2} + \frac{\partial^2 T}{\partial y^2} \right) + \mu \phi \quad (5)$$

$$\phi = 2 \left[ \left( \frac{\partial u}{\partial x} \right)^2 + 2 \left( \frac{\partial v}{\partial y} \right)^2 + 2 \left( \frac{\partial w}{\partial z} \right)^2 + \left( \frac{\partial u}{\partial y} + \frac{\partial v}{\partial x} \right)^2 + \left( \frac{\partial u}{\partial z} + \frac{\partial w}{\partial x} \right)^2 + \left( \frac{\partial v}{\partial z} + \frac{\partial w}{\partial y} \right)^2 \right] \quad (6)$$

$\nu$ : is the kinematic viscosity of the fluid (m<sup>2</sup>/s),  $k$ : thermal conductivity (w/m.k).  $C_p$ : Specific heat capacity at constant pressure (j/kg.k).

### 2.2 Discrete Phase Model (DPM)

ANSYS Program 15 predicts the trajectory of a discrete phase particle (droplet or bubble) by integrating the force balance on the particle, which is written in a Lagrangian reference frame. This force balance equates the particle inertia with the forces acting on the particle, and can be written as:

$$\frac{d\vec{u}_p}{dt} = F_D(\vec{u} - \vec{u}_p) + \frac{\vec{g}(\rho_p - \rho)}{\rho_p} + \vec{F} \quad (7)$$

where  $\vec{F}$  is an additional acceleration (force/unit particle mass).

Term,  $F_D(\vec{u} - \vec{u}_p)$  is the drag force per unit particle mass, which is defined as following:

$$F_D = \frac{18 \mu C_D Re}{\rho_p d_p^2 24} \quad (8)$$

$$C_d = \frac{2 F_d}{\rho u^2 A} \quad (9)$$

where  $F_d$ : Newton (kg.m/s<sup>2</sup>),  $C_d$ : drag force coefficient a dimensionless number,  $\mu$ : molecular viscosity of the fluid (Pa·s or N·s/m<sup>2</sup> or kg/m·s),  $Re$  is the relative Reynolds number a dimensionless number,  $\vec{U}$  is the fluid phase velocity (m/s),  $\vec{u}_p$  is the particle velocity (m/s),  $\rho$  is the fluid density,  $\rho_p$  is the density of the particle (Kg/m<sup>3</sup>), and  $d_p$  is the particle diameter ( $\mu m$ ).

A discrete particle model option was used to model the movement of the particles in the surgical operation room. This option allows the CFD analysis to predict the trajectory movement of the particles resulting from the air flow pattern. In this study the particles were assumed to be released with inlet air supply from the (SOR).

The discretization of the domain is led to reduce the previous equations to their finite volume domain form. The standard turbulence model is applied and there are many heat sources in the surgical operation room [SOR]: such as the medical equipments, lamps, patients and the surgical staffs who are working during the operation. Many researchers did not consider the surgical staffs and patient as heat sources because they claim that the simplified model of them has less surface area than the actual body area. Also, by considering them as heat sources would produce a high localized temperature around the people's model [7]. Heat and turbulence were created a buoyancy driven airflow that flows upwards depending on the temperature difference [3].

The magnitude of heat generated from medical equipments and lamps can be obtained from the specification of the equipments. Equipments such as the main medical lamp and the satellite medical lamp release heat at a rate of approximately 350 W and 200W, respectively. Surgical staffs and patient release heat in the range of 100 to 150W. The patient usually produces the least amount of heat while the surgeon generates the highest amount of heat [8].

In this study, a general purpose computational fluid dynamics (CFD) software ANSYS CFX-15 was used to develop model of the surgical operation room (SOR) in the general al Najaf hospital.

The operation room was (7m long, 6.3m width and 3m height) as shown in Table 1. The model comprises of an operating table placed in the middle section of the room, one patient on the table, one glass window and one door. Also included are four surgical staff distributed one person on each side of the operating table. They are represented by cubic geometries. One surgical lamp is also included in the model, which was suspending from ceiling with one patient on the operation table and four ceiling lights. Figure 1 shows the studied surgical operation room as presented by program.

Turbulence is air flow supplied by a diffuser located in the room ceiling, and the flow air is directed straightaway on the operation table. There are four outlets located on the walls at distance (0.25m) from floor. The flow air is considered to be incompressible in the actual case simulation. the air velocity is specified by 0.28 m/s, and a zero pressure state is prescribed on the four outlets on the room walls, which

represents an atmospheric pressure, Also, A no slip flow conditions is prescribed on the walls, , and this will simplify the CFD analysis. Heat transfer analysis is turned-on by activating the energy equation feature. This will ensure that the effect of heat dissipated from the surgical lamp, patient, windows and staffs would be taken into account during the computations [8]. In this study, a three-dimensional tetrahedral elements is used. The model configurations were set, so that, getting a best convergence among grid, dependent, and runtime saving, because of the difficult domain geometry as shown in Figure 2.

The standard k-ε turbulent model was chosen for the flow analysis. 5% turbulent intensity is selected for CFD analysis. The CFD program is operated by using finite volume method. The convergence criterion was  $1 \times 10^{-4}$ .

Table 1. The contents and dimensions in the surgical operation room.

Objects	The size (m)(L,H,W)	The number
supply air inlet	2.5(L)x1.25(W)	1
Exit air outlet	0.6(H)x0.4(W)	4
door	2(H)x1(W)	1
window	1.5(H)x1.5(W)	1
Patient	1.75(L)x0.7(W)x0.3(H)	1
Surgical staff	0.4(L)x0.7(W)x1.75(H)	4
Operation table	1.8(L)x1.2(W)x0.5(H)	1
Ceiling lamps	0.6(L)x0.6(W)	4
Surgical lamps	D=1.25, t=0.25	1
Equipment 1	1(L)x0.5(W)x0.5(H)	1
Equipment 2	1.5(L)x0.5(W)x0.5(H)	1

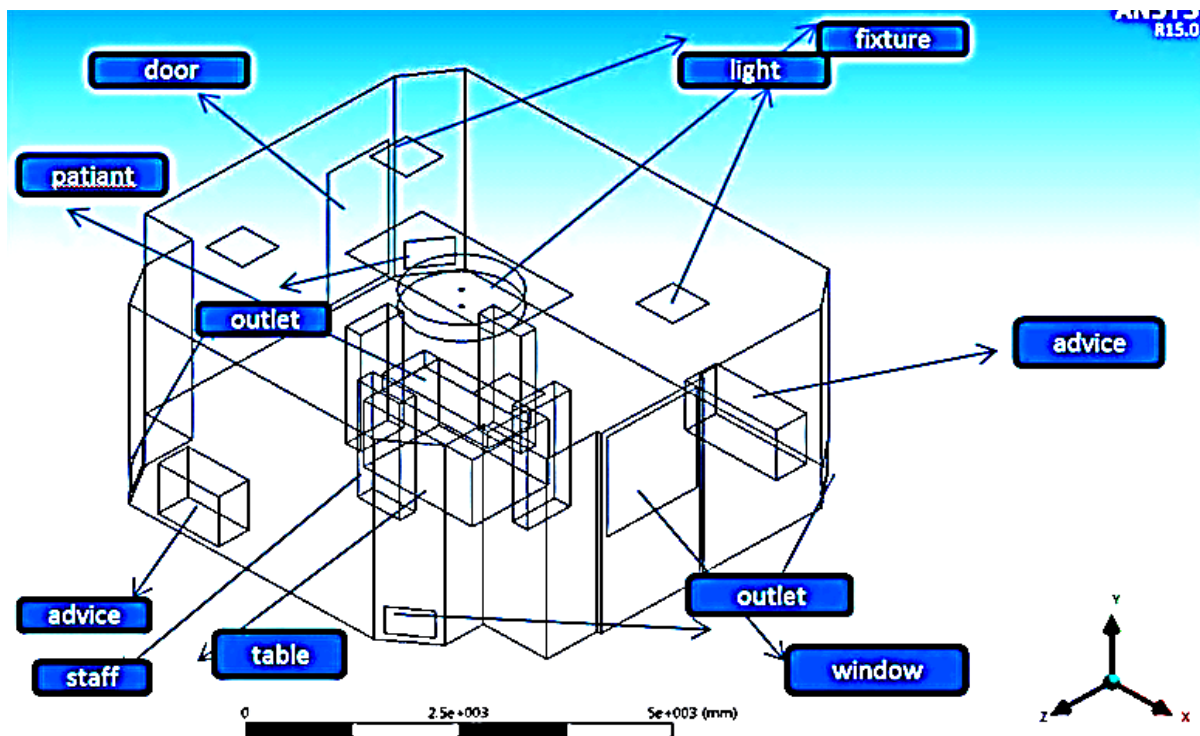


Figure 1. Operating room.

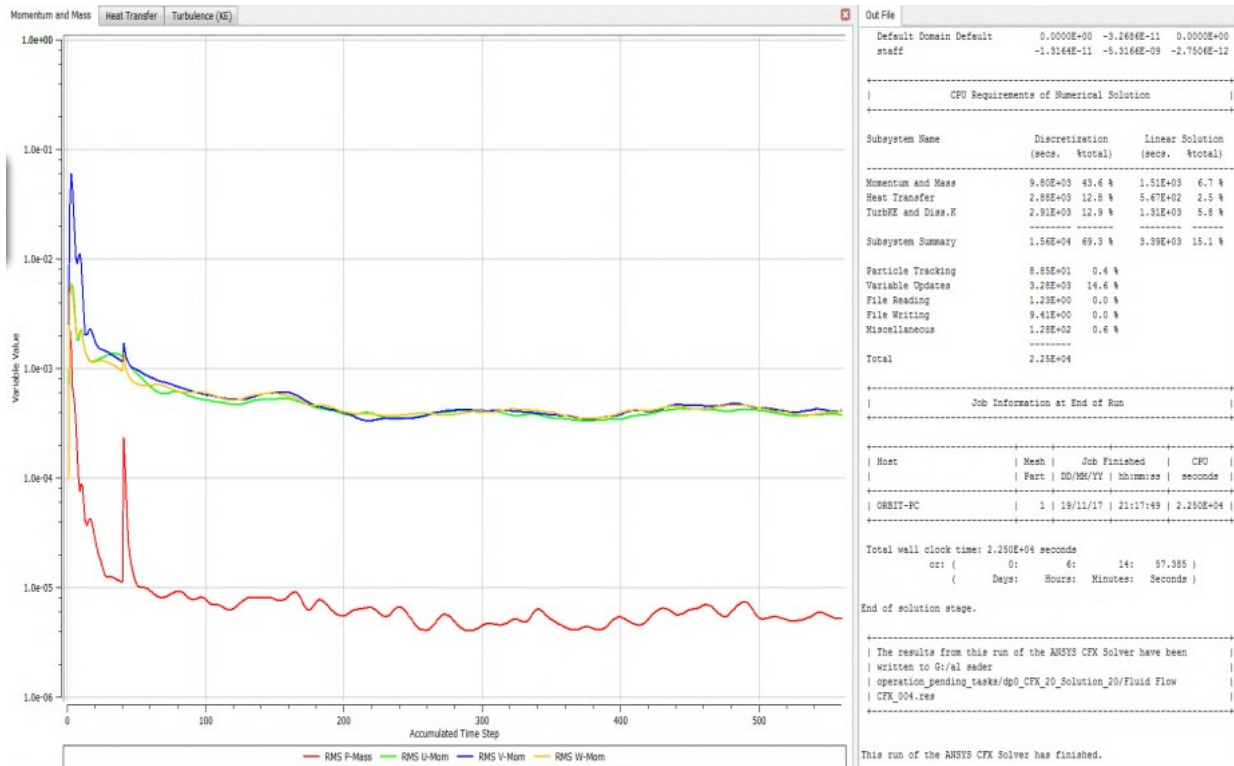


Figure 2. Mesh independent study.

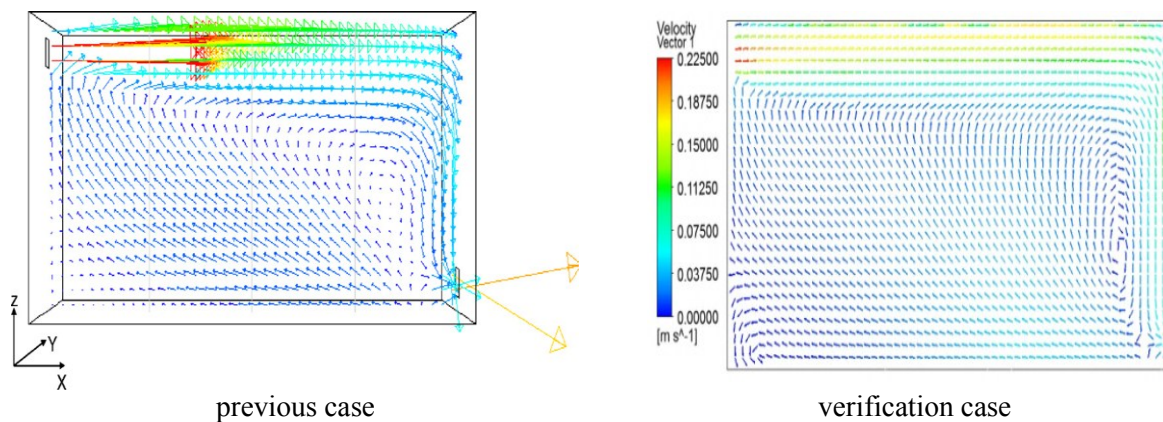
**3. Results and discussion**

**3.1 Verification case**

In this study as a first step, the appropriated ANSYS 15 program is validated against the results of the work reported by Chen, F. et, al [1]. In this work the governing equations, namely, mass conservation, momentum, energy and concentration, were solved using Ansys (Fluent 2005) program, for turbulent airflow inside a chamber of dimensions (L = 0.8m, W = 0.4m, H = 0.4 m). The following air was contaminated with particles at different concentrations.

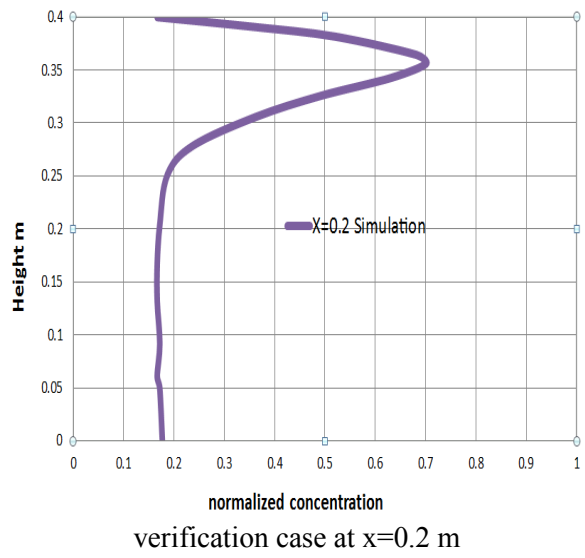
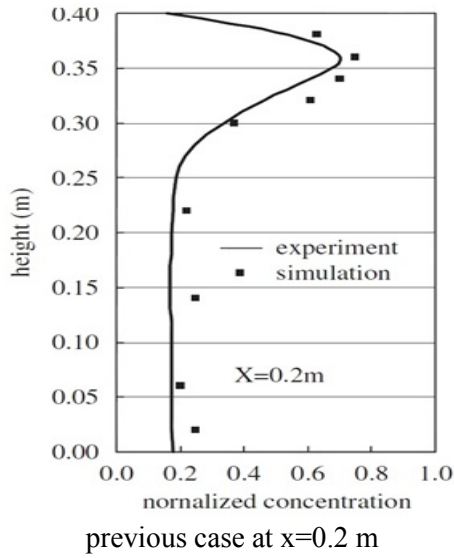
In the current study a similar model to that given in [1], is designed using the ANSYS 15 program, and the governing equations previously stated are solved using the same program.

The results of both studied are shown in Figure 3. These results represent the velocity distribution, and particle concentrations at different locations in the chamber. It can be observed that there is a reasonable matching between the previous and current results.

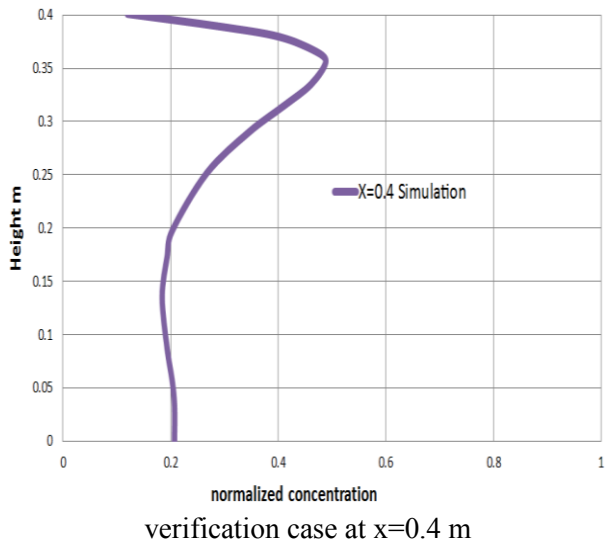
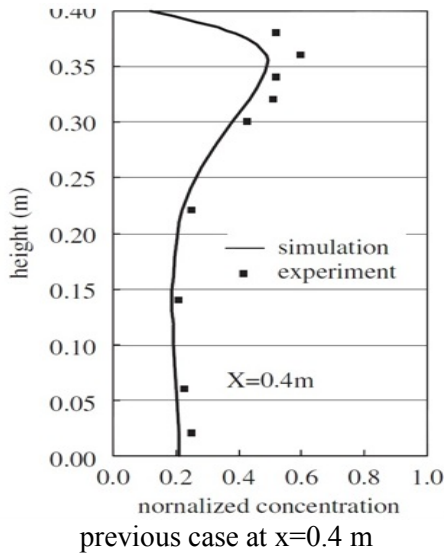


(a) Velocity vector

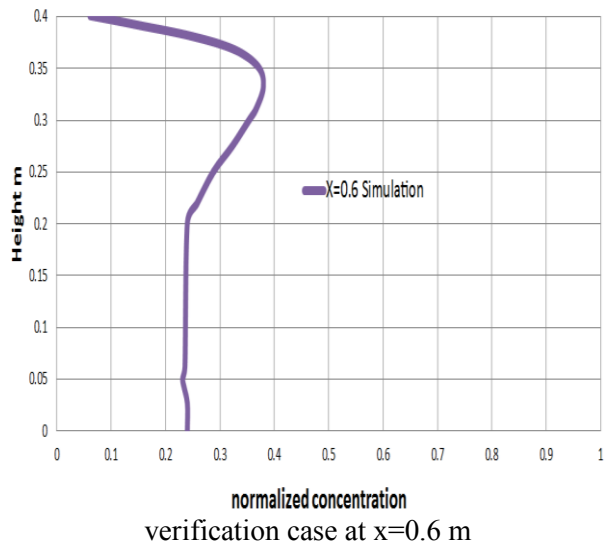
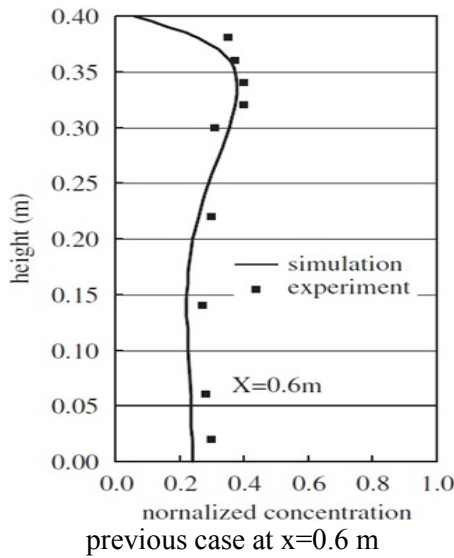
Figure 3. Continued.



(b) Particle concentration



(c) Particle concentration



(d) Particle concentration

Figure 3. A comparison between the results of the previous research and verification case.

### 3.2 Studied cases

In this research a surgical operation room (SOR) of AL-Najaf hospital is considered to be studied under its actual conditions and under two other improved cases.

#### 3.2.1 Actual case

The (SOR) is of (7m x 6.3m x 3m height). The conditioned air is supplied to the room from its ceiling by one simple slot of (2.5m x 1.25m) size. The amount of supplied air is 3150 m<sup>3</sup>/hr corresponding to 25 ACH (air change per hour). The inlet air is of 0.28 m/s velocity and 293 k temperature. No filter is maintained in the inlet so that there are airborne particles introducing to the room with supplied air as shown in Table 2. The contaminant air is exhausted air from the room through four grills of (0.6m x 0.4m) size, fixed in the walls at the distance of 0.25m from the floor. The operation room consists of an the operation table with a patient lying on it, four staffs standing near the operation table and emitting 150 W convective heat each, operation lights emitting 150w, and ceiling lights and some other equipments emitting a total heat of 380 W. The boundary conditions of heat transfer for all the walls, ceiling and floor are set to be adiabatic. The surface temperature of the patient is assumed to be affected by the radiation heat of the operation lights, and this will not result in an important influence on the air distribution. It is assumed that there is no relative velocity between the particles and the air carrying the particles. The computed field distributions of this case included the following:

1. The air velocity and temperature distribution along a vertical line between supplied air and the floor in the (SOR) as shown in Figures 4 and 5. These figures, show that the air high velocity values near the supply opening, and high temperature values near the region of the surgical lights in the middle area of the operation room because of finding the surgical lights and staffs under the supply air slot at distance one meter below the ceiling of (SOR).
2. The air velocity, temperature and particle concentration as shown in Figures 6-8. Figure 6 shows that the existed ventilation system gives a vertical unidirectional flow above the operation area. The air temperature difference in the room is small due to the available heat sources as lights, staffs, patient and surgical lights. The particle concentration contours are plotted for a section in the (SOR) as shown in Figure 8. The results shown that very low concentration of particles in the operation area, and high concentration in the vicinity of the surgical lights. The transportation of particles in the rest of the room depends on the source location and airflow patterns.
3. The velocity vectors are plotted for the vertical mid-section of the (SOR) as shown in Figure 9. It is clear that the effect of surgical light under supply air opening leads to air flow diffusion toward the walls.

#### 3.2.2 Assumed case (1)

In this case the air flow rate is assumed to be 5017 m<sup>3</sup>/hr corresponding to an air change per hour of (40 ACH). The air inlet velocity is 0.446 m/s. The results of this case including the air velocity and temperature distributions, contours and velocity vectors are shown in Figures 10-15 respectively. These plots have the same trend as for the actual case.

It can be observed from these results that, when increasing the air flow rate the average temperature of the SOR is decreased by an amount of 5 °k, and the particle concentrations are also decreased due to higher inlet air velocity. Higher inlet velocity decreases the time necessary for air heating near the heat sources and in the same time facilitate the process of pulling away the particles.

Table 2. The particles physical properties.

Define Particle Data	Particle Solids (Rubber type)
Mass And Momentum	Normal Speed
Normal Speed	2.8000e-01 [m s <sup>-1</sup> ]
Particle Diameter Distribution	Specified Diameter
Diameter	5.0000e+00 [micron]
Mass Flow Rate	6.4000e-08 [kg s <sup>-1</sup> ]
Particle Position	Uniform Injection
Number	5.0000e+04
Number of Positions	Direct Specification
density	1100kg/m <sup>3</sup>
Morphology	Dispersed Particle Transport Solid

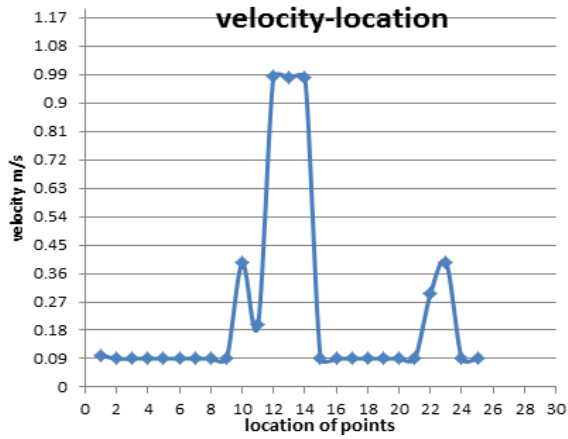


Figure 4. Curve V–Location for real case

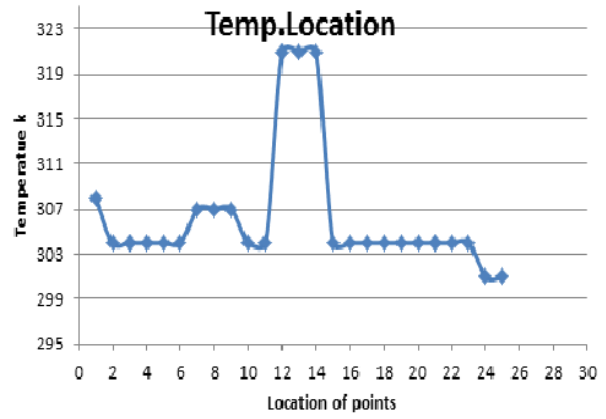


Figure 5. Curve T–Location for real case

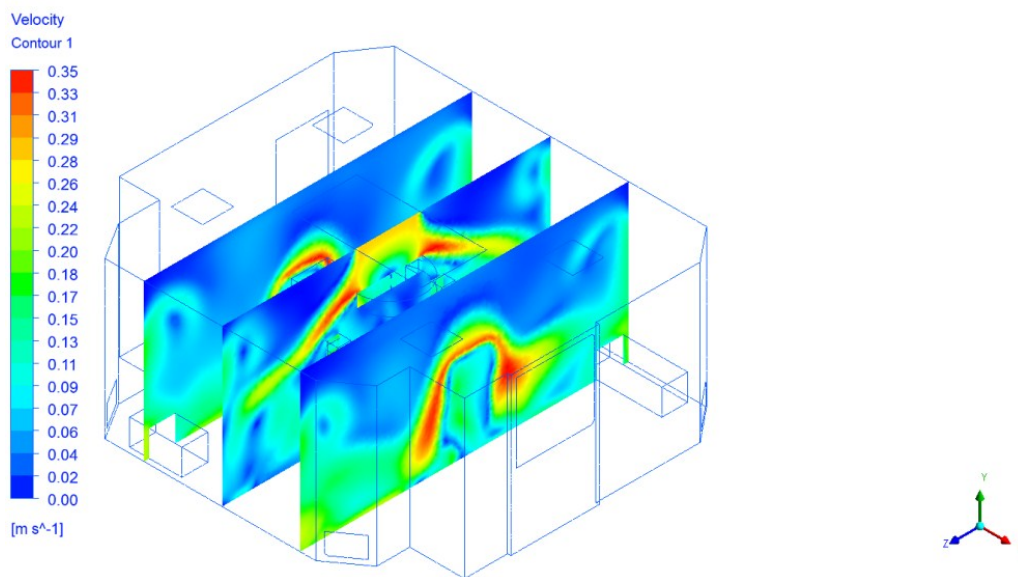


Figure 6. Contour of velocity values (real case) y-z plane.

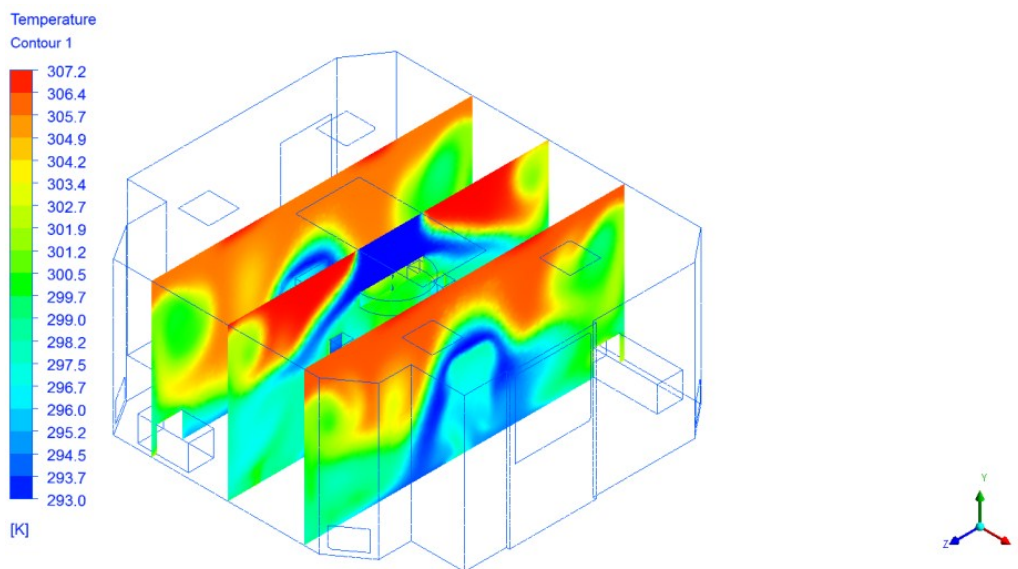


Figure 7. Contour of Temperature values(real case) y-z plane.

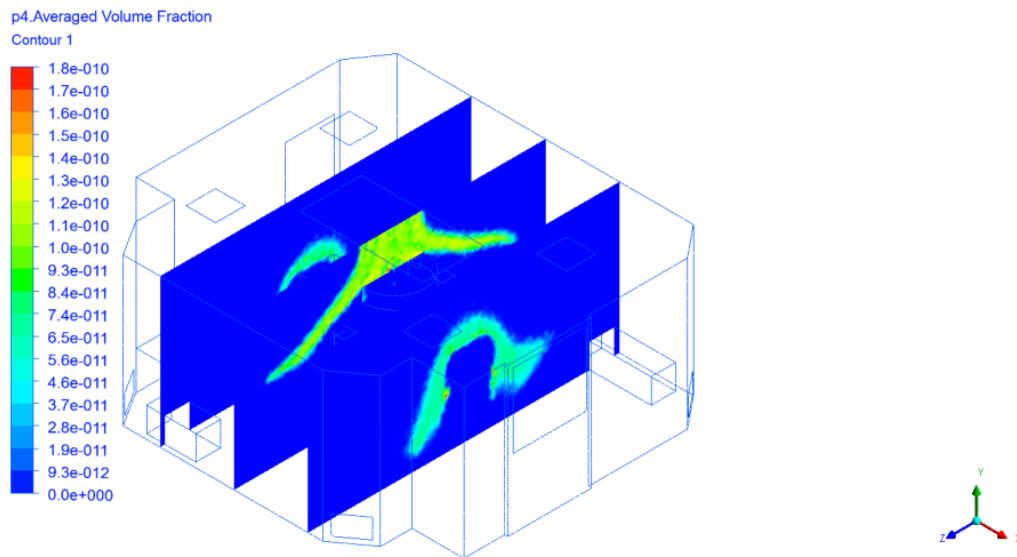


Figure 8. Contour of particle concentration values (real case) y-z plane.

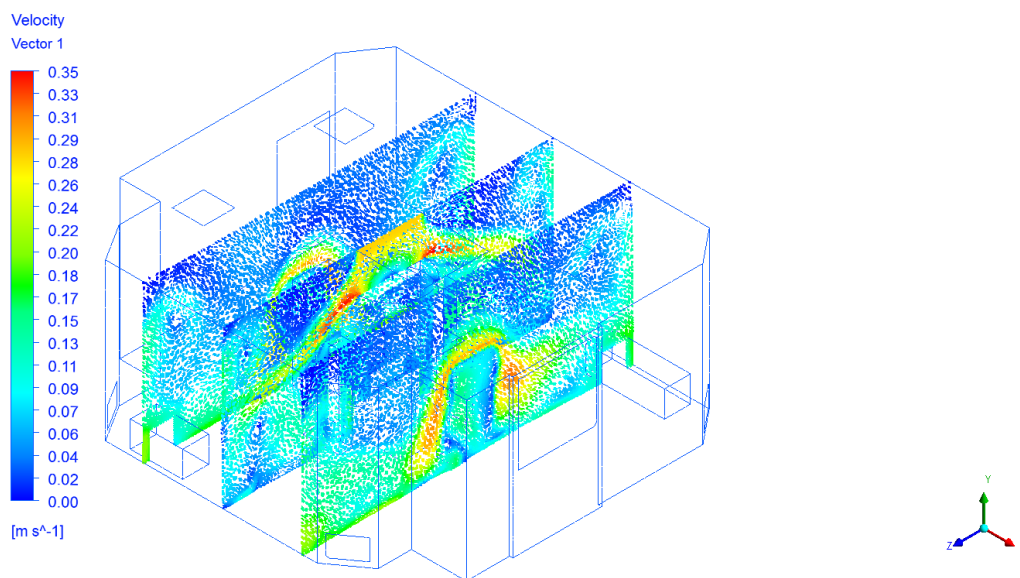


Figure 9. Velocity vector on (real case) y-z plane.

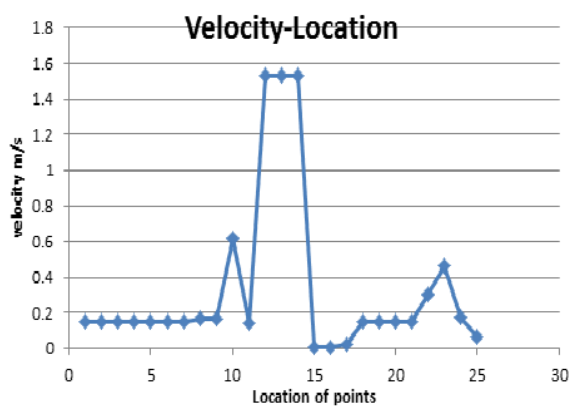


Figure 10. Curve V–Location for case 1.

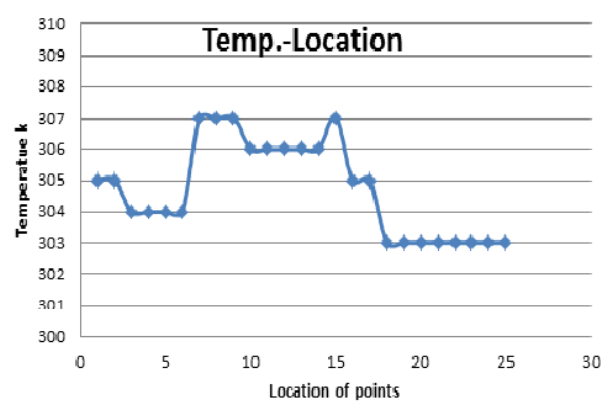


Figure 11. Curve T–Location for case 1.

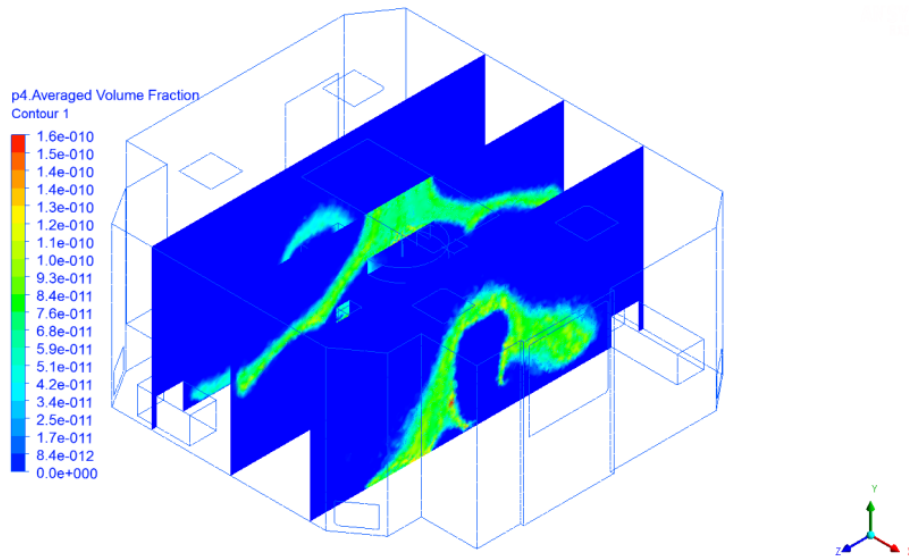


Figure 12. Contour of particle concentration values (case 1) y-z plane.

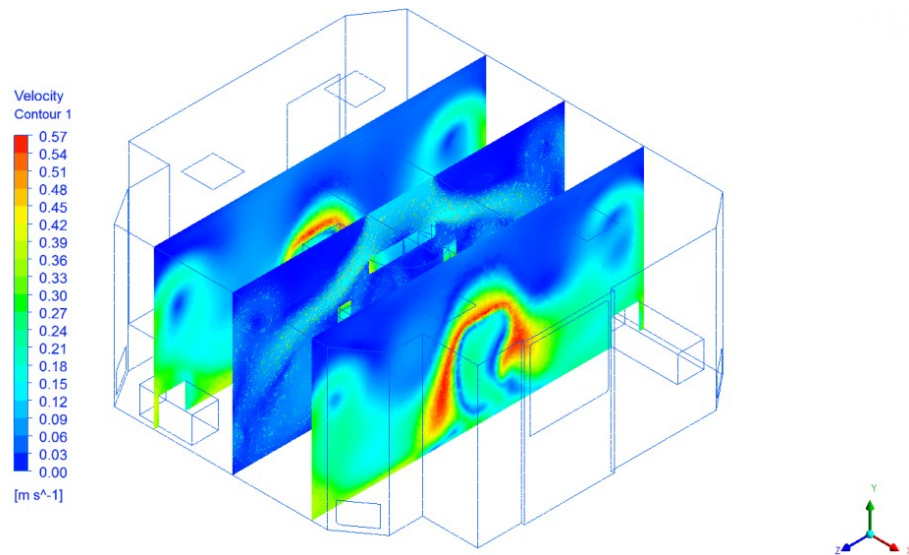


Figure 13. Contour of velocity values (case 1) y-z plane.

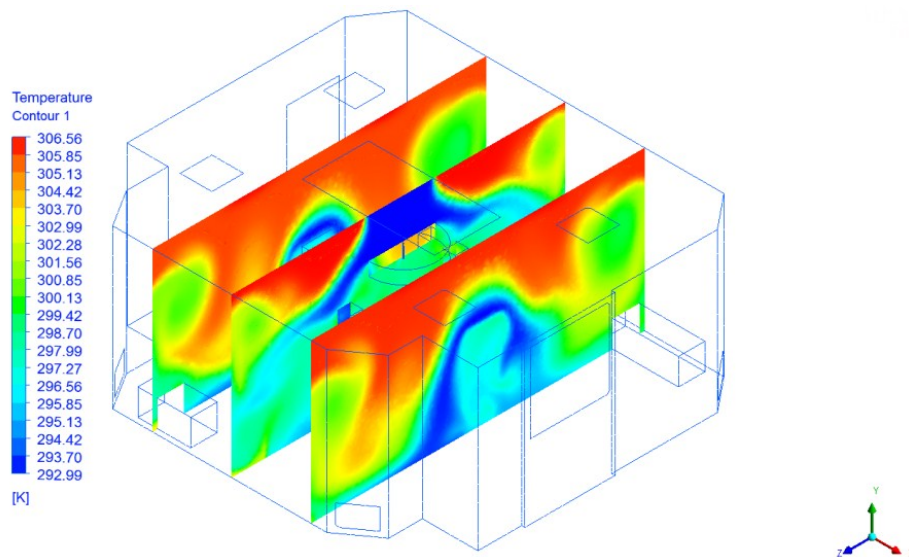


Figure 14. Contour of temperature values (case 1) y-z plane.

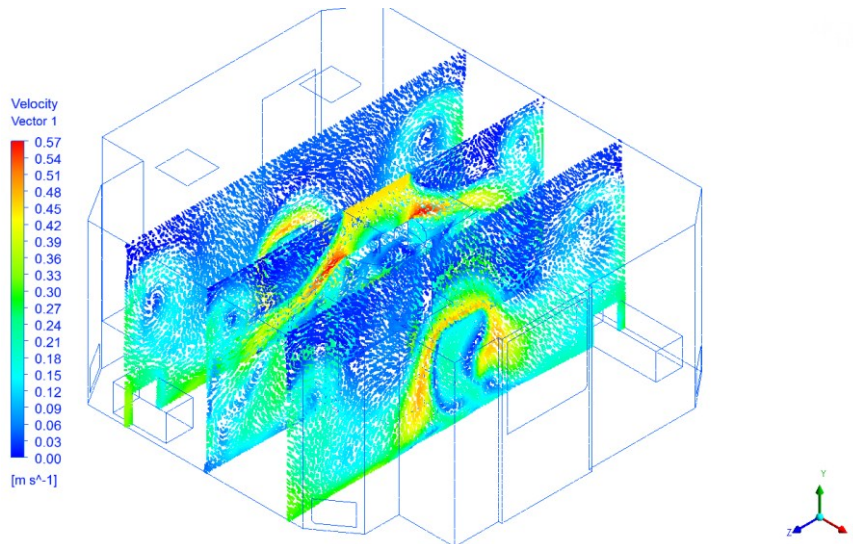


Figure 15. Velocity vector on (case 1) y-z plane.

3.2.3 Assumed case (2)

The air flow rate in this case is assumed to be 7560 m<sup>3</sup>/hr corresponding to (60 ACH). The inlet air velocity is 0.672 m/s. The results of this case including the air velocity and temperature distributions, contours, and velocity vectors are shown in Figures 16-21 respectively. As for the previous case, higher inlet air velocity decreased the room average temperature by 6 °k, as compared with the actual case, and also decreased the particle concentration in the operation area of the (SOR). It should be noted also that increasing the supplied air flow may affect the comfortable environment of the occupants, because of decreasing the indoor temperature. The numerical results of the above three cases are listed in Table 3.

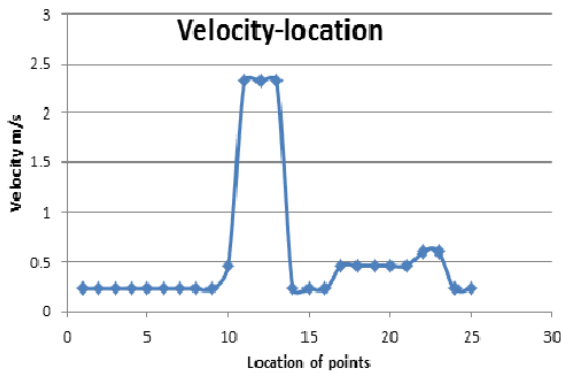


Figure 16. Curve V–location for case 2.

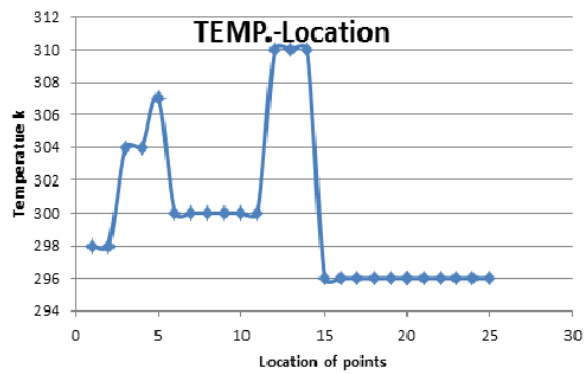


Figure 17. Curve T–location for case 2.

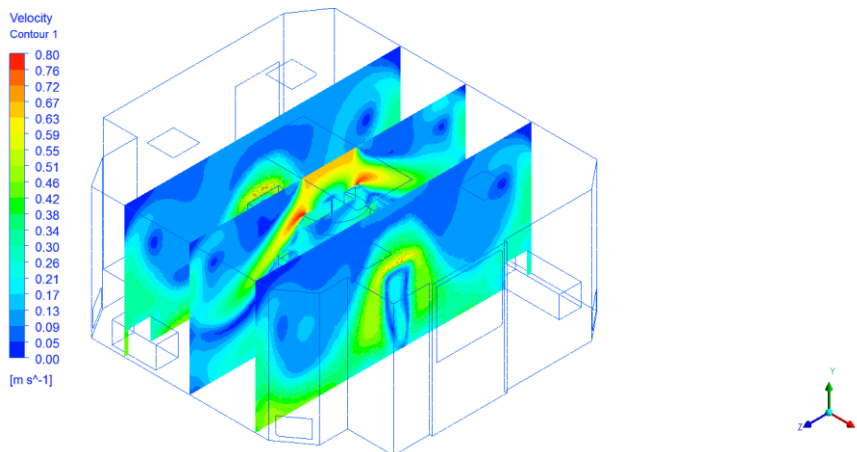


Figure 18. Contour of velocity values (case 2) y-z plane.

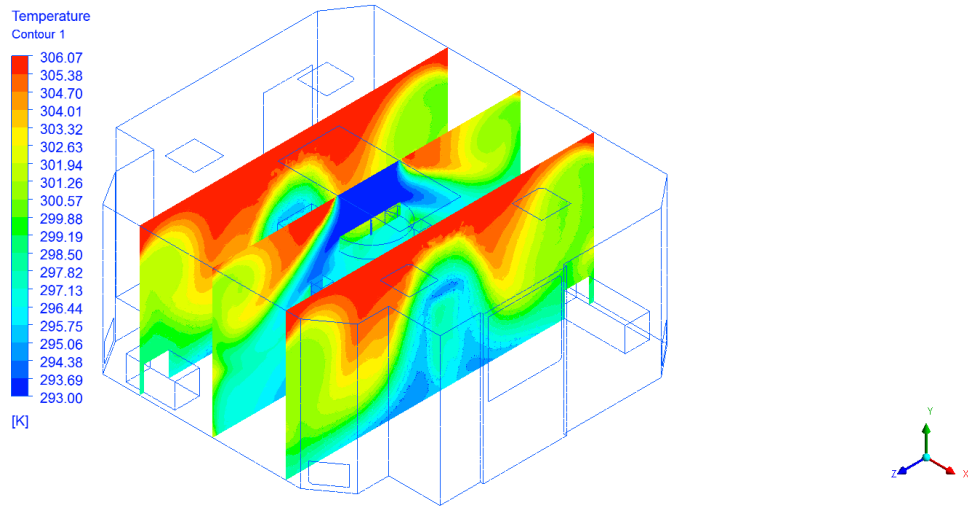


Figure 19. Contour of Temperature values (case 2) y-z plane

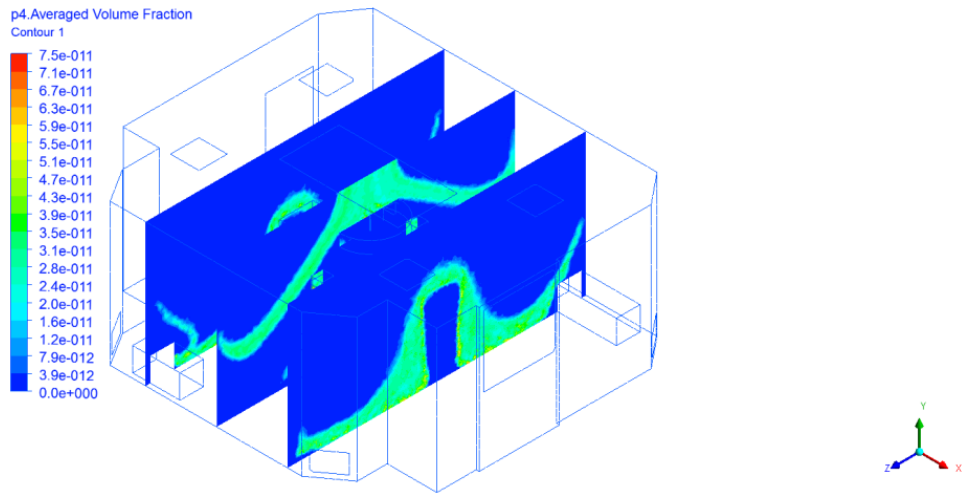


Figure 20. Contour of particle concentration values (case 2) y-z plane.

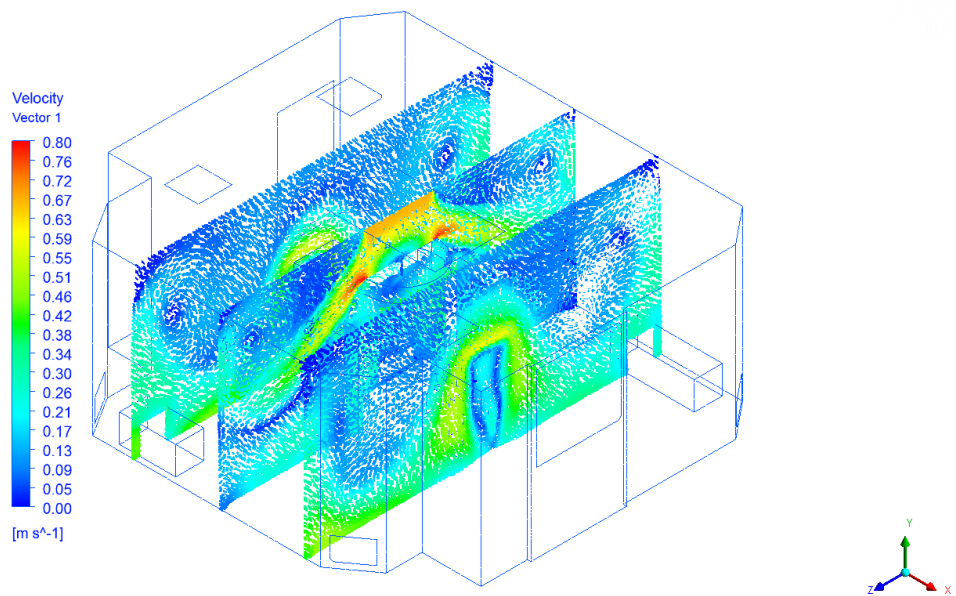


Figure 21. Velocity vector on (case 2) y-z plane.

Table 3. Numerical values of air velocity, temperature and particle concentration of different points in the domain for the studied cases.

Point	Location			Numerical (actual case)			Numerical (case1)			Numerical (case2)		
	X	Y	Z	V(m/s)	T(k)	PC	V(m/s)	T(k)	PC	V(m/s)	T(k)	PC
1	3	3	-18	0.1	308	5.78e <sup>-011</sup>	0.15	305	3.8e <sup>-011</sup>	0.23	298	3.8e <sup>-011</sup>
2	3	3	-19	0.09	304	5.78e <sup>-011</sup>	0.15	305	3.8e <sup>-011</sup>	0.23	298	3.8e <sup>-011</sup>
3	3	3	-20	0.09	304	5.78e <sup>-011</sup>	0.15	304	3.8e <sup>-011</sup>	0.23	304	3.8e <sup>-011</sup>
4	3	3	-21	0.09	304	5.78e <sup>-011</sup>	0.15	304	3.8e <sup>-011</sup>	0.23	304	3.8e <sup>-011</sup>
5	3	3	-22	0.09	304	5.78e <sup>-011</sup>	0.15	304	3.78e <sup>-011</sup>	0.23	307	3.78e <sup>-011</sup>
6	3	2.5	-22	0.09	304	5.78e <sup>-011</sup>	0.15	304	3.8e <sup>-011</sup>	0.23	300	3.8e <sup>-011</sup>
7	3	2	-22	0.09	307	5.78e <sup>-011</sup>	0.15	307	3.8e <sup>-011</sup>	0.23	300	3.8e <sup>-011</sup>
8	3	1.5	-22	0.09	307	5.78e <sup>-011</sup>	0.17	307	3.8e <sup>-011</sup>	0.23	300	3.8e <sup>-011</sup>
9	3	1	-22	0.09	307	5.78e <sup>-011</sup>	0.17	307	3.8e <sup>-011</sup>	0.23	300	3.8e <sup>-011</sup>
10	3	0.5	-22	0.393	304	5.78e <sup>-011</sup>	0.62	306	3.8e <sup>-011</sup>	0.464	300	3.8e <sup>-011</sup>
11	3	0	-22	0.197	304	5.78e <sup>-011</sup>	0.146	306	3.8e <sup>-011</sup>	0.464	300	3.8e <sup>-011</sup>
12	2.5	0	-22	0.983	321	5.78e <sup>-010</sup>	1.53	306	3.8e <sup>-010</sup>	2.32	310	3.8e <sup>-010</sup>
13	2	0	-22	0.983	321	5.78e <sup>-010</sup>	1.53	306	3.8e <sup>-010</sup>	2.32	310	3.8e <sup>-010</sup>
14	1.5	0	-22	0.983	321	5.78e <sup>-010</sup>	1.53	306	3.8e <sup>-010</sup>	2.32	310	3.8e <sup>-010</sup>
15	1	0	-22	0.09	304	5.78e <sup>-011</sup>	0.007	307	3.8e <sup>-011</sup>	0.23	296	3.8e <sup>-011</sup>
16	0.5	0	-22	0.09	304	5.78e <sup>-011</sup>	0.009	305	3.8e <sup>-011</sup>	0.23	296	3.8e <sup>-011</sup>
17	0	0	-22	0.09	304	5.78e <sup>-011</sup>	0.024	305	3.8e <sup>-011</sup>	0.23	296	3.8e <sup>-011</sup>
18	-0.5	0	-22	0.09	304	5.78e <sup>-011</sup>	0.15	303	3.8e <sup>-011</sup>	0.464	296	3.8e <sup>-011</sup>
19	-1	0	-22	0.09	304	5.78e <sup>-011</sup>	0.15	303	3.8e <sup>-011</sup>	0.464	296	3.8e <sup>-011</sup>
20	-1.5	0	-22	0.09	304	5.78e <sup>-011</sup>	0.15	303	3.8e <sup>-011</sup>	0.464	296	3.8e <sup>-011</sup>
21	-2	0	-22	0.09	304	5.78e <sup>-011</sup>	0.15	303	3.8e <sup>-011</sup>	0.464	296	3.8e <sup>-011</sup>
22	-2.5	0	-22	0.295	304	5.78e <sup>-011</sup>	0.3	303	3.8e <sup>-011</sup>	0.6	296	3.8e <sup>-011</sup>
23	-3	0	-22	0.393	304	5.78e <sup>-011</sup>	0.46	303	3.8e <sup>-011</sup>	0.6	296	3.8e <sup>-011</sup>
24	0.07	1.5	-19.15	0.09	301	5.78e <sup>-011</sup>	0.175	303	3.8e <sup>-011</sup>	0.23	296	3.8e <sup>-011</sup>
25	0.07	0.93	-19.15	0.09	301	5.78e <sup>-011</sup>	0.063	303	3.8e <sup>-011</sup>	0.23	296	3.8e <sup>-011</sup>

#### 4. Conclusions

Three dimensional study of air flow in a (SOR) with ceiling supply and side exhaust grills is studied. The effect of air change per hour (ACH) is investigated. It is shown that ACH affect the velocity, temperature, and particle concentration distribution in the (SOR). With increasing ACH the average indoor temperature is decreased, and the concentration of contaminant particles is also decreased specially around the operation table where the patient is lying on. With higher values of ACH the average indoor temperature is more decreased, which is an undesired conditions when considering the comfortable requirements. As shown in Table 4.

Increasing ACH leads to decrease particle concentration in some other zones of the room because of formation of some particle vortices.

Table 4. Numerical average of air velocity, temperature and particle concentration of different points in the domain for the studied cases.

ACH	Average velocity [m/s]	Average temperature [ $K^{\circ}$ ]	Average particle concentration
25	0.242	306.32	$7.34 \times 10^{-11}$
40	0.335	304.72	$4.86 \times 10^{-11}$
60	0.567	299.88	$4.80 \times 10^{-11}$

#### Reference

- [1] Chen, F., Yu, S.C.M., Lai, A.C.K., Modeling particle distribution and deposition in indoor environments with a new drift-flux model. *Atmospheric Environment* 2006, pp.357-367
- [2] ISO 14644-8:2006 Cleanrooms and associated controlled environments. Classification of airborne molecular contamination

- [3] Junjie Liu, H.W., Wenyong Wen, Numerical simulation on a horizontal airflow for airborne particles control in hospital operating room. *Building and Environment*, 2009, pp. 2284-2289.
- [4] Wirtanen, G., Miettinen, H., Pahkala, S., Enbom, S. & Vanes, L. Clean air solutions in food processing. <http://www.vtt.fi/inf/pdf/publications/2002/P482.pdf>
- [5] Schicht, H.H. Cleanroom technology and its benefits to the food and beverage industry. *New Food*, (1999), 1, 18-23.
- [6] Whyte, W. Cleanroom technology, Fundamentals of design, testing and operation. John Wiley & Sons Ltd., Chichester, 2001.
- [7] Zhang Rui, T.G., Ling Jihong, Study on biological contaminant control strategies under different ventilation models in hospital operating room. *Building and Environment* 2008. 43: pp.793-803.
- [8] Haslinda M. K "Analysis of Air and Airborne Particles Movements in a Hospital Operating Theater" *Journal of Advanced Review on Scientific Research* 2014, 4(1), pp.20-30.